Electrostatic Energy-Harvesting and Battery-Charging CMOS System Prototype

Erick O. Torres, *Graduate Student Member, IEEE*, and Gabriel A. Rincón-Mora, *Senior Member, IEEE*

***Abstract*—The self-powering, long-lasting, and functional features of embedded wireless micro-sensors appeal to an ever-expanding application space in monitoring, control, and diagnosis for military, commercial, industrial, space, and biomedical applications. Extended operational life, however, is difficult to achieve when power-intensive functions like telemetry draw whatever little energy is available from energy-storage micro-devices like thin-film lithium-ion batteries and/or micro-scale fuel cells. Harvesting ambient energy overcomes this deficit by continually replenishing the energy reservoir and indefinitely extending system lifetime. In this paper, a prototyped circuit that pre-charges, detects, and synchronizes to a variable voltage-constrained capacitor verifies experimentally that harvesting energy electrostatically from vibrations is possible. Experimental results show that, on average (excluding gate-drive and control losses), the system harvests 9.7 nJ/cycle by investing 1.7 nJ/cycle, yielding a net energy gain of approximately 8 nJ/cycle at an average of 1.6 µW (in typical applications) for every 200 pF variation. Projecting and including reasonable gate-drive and controller losses reduces the net energy gain to 6.9 nJ/cycle at 1.38 µW.**

***Index Terms*— Batteries, energy harvesting, micro-sensors, self-powered, self-sustaining, vibration energy harvester.**

I. Electrostatic Energy Harvesting

SELF-POWERED micro-systems, such as wireless transceiver micro-sensors [1], biomedical implants [2]-[4], military monitoring devices [5], and structure-embedded instrumentation [6], support power-hungry functions like transmission and data conversion from miniaturized sources. This combination, when conformed to micro-scale dimensions, results in limited and finite operational lifetimes because micro-scale energy-storage devices cannot store sufficient energy to sustain various system tasks for long. State-of-the-art thin-film lithium-ion batteries (Li Ion) [7] and direct-methanol proton-exchange membrane (DM-PEM) fuel cells [8] exhibit promising but finite energy densities that, when coupled with improved power-efficient designs, low duty-cycle multiplexing, and smart power-aware network protocols [1], help extend life, but only as much as volume allows.

Scavenging ambient energy overcomes this space constraint by restocking the system with energy *in situ*, within the device, as shown in Figure 1, from energy that would otherwise be lost [9]-[12]. Concurrently scavenging and consuming energy can extend operational lifetime indefinitely by automatically replenishing what is lost, outperforming both state-of-the-art Li Ion and DM-PEM fuel-cell technologies, and any hybrid combination thereof. Harvesting, however, requires energy and producing a net gain (i.e., harvested energy minus energy required to scavenge) in a practical system is challenging, and research in this area is still in its infancy.

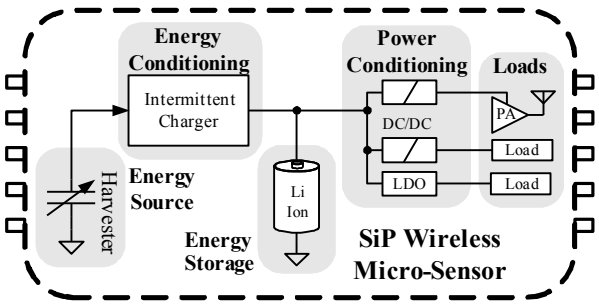

Figure 1. System-in-package (SiP) wireless micro-sensor system.

Nevertheless, of the available energy sources, which include light [13]-[14], thermal gradients [15]-[17], and motion [18]-[21], the latter, in the form of vibrations, is arguably most abundant, stable, and predictable in practical applications. While converting and conditioning this energy to electrical power is possible by harnessing the damping forces produced by magnetic fields [22]-[26], electric fields [27]-[28], and strain on piezoelectric materials [29]-[34], electrostatic means are probably most compatible with CMOS integration because the harvesting device is a relatively simple variable plate-distance capacitor built with standard micro-electromechanical systems (MEMS) technologies.

Fundamentally, electrostatic harvesters harness the work ambient vibrations exert on the electrostatic force of a variable capacitor (i.e., varactor). In more physical terms, vibrations cause the gap distance and/or overlap area of a parallel-plate capacitor (C_{VAR}) to vary [11] with a net effect, under constant charge or voltage conditions, of producing electrical energy [27]. When constraining charge by keeping the capacitor open circuited, voltage increases with decreasing capacitance

Manuscript received July 2, 2008 and revised September 30, 2008. This work is supported by the Texas Instruments Analog Fellowship Program.

E. O. Torres and G. A. Rincón-Mora are with the Georgia Tech Analog, Power, and Energy IC Research Lab, School of Electrical and Computer Engineering, Georgia Institute of Technology, Atlanta, GA 30332-0250 USA (e-mail: ertorres@ece.gatech.edu, rincon-mora@ece.gatech.edu).

($Q_{CONSTANT} = C_{VAR}V$), increasing the potential energy stored in the capacitor; the increasing squared effects of voltage on energy offset the decreasing linear effects of capacitance (i.e., $E_{CAP} = \frac{1}{2}CV^2$). Similarly, by constraining voltage, the mechanical energy moving the capacitor plates drives charge out of the capacitor, yielding a net harvesting current i_{HARV} ($Q = C_{VAR}V_{CONSTANT}$)

$$i_{HARV} = \frac{dQ}{dt} = C\frac{\partial V}{\partial t} + V\frac{\partial C}{\partial t} = V\frac{\partial C}{\partial t}. \quad (1)$$

The maximum voltages charge-constrained systems produce, however, surpass the breakdown limits of most modern CMOS technologies by a considerable margin. A 1-200 pF variation, for instance, amplifies the initial voltage across C_{VAR} by a factor of 200, by its maximum-minimum capacitance ratio [35]-[38], producing peak voltages of roughly 25-200 V from inputs as low as 125 mV to 1 V. More costly and specialized technologies, such as silicon-on-insulator (SOI) CMOS processes [37]-[38], can sustain these voltage extremes but their increased costs limit the extent to which the market will adopt them, especially in wireless micro-sensors where volume production and low cost are driving factors.

Constraining the voltage may keep voltage excursions within tolerable levels but also requires an additional voltage source [11], [27], which conflicts with integration. Another possibility is to embed a material that has permanent charge separation in a dielectric and thus a constant voltage, as in the case of electrets and charged electrodes [39]-[42], except they require either a complicated assembly process to integrate two separate substrates, one being the electret, or additional fabrication sequences to charge the material via electron tunneling. References [43] and [44] use a storage capacitor to constrain voltage but the capacitor is not a true low-impedance source so its voltage changes, which is why the capacitor undergoes a charge-constrained phase that leaves otherwise useful energy unharvested in the variable capacitor, as only a small fraction of the full capacitance variation is now harvested.

In the proposed system, the voltage across the capacitor is held constant by the already-existing energy-storage device (i.e., the rechargeable battery), the one ultimately receiving the harvested energy. In this way, the harvester avoids the use of additional voltage sources, as mentioned in [11] and [27]. The key contribution of this paper is how the proposed and prototyped circuit (which pre-charges, detects, and synchronizes to a variable voltage-constrained capacitor) verifies experimentally that harvesting energy electrostatically from vibrations is possible. Sections II and III describe the basic concept, design, and implementation of the proposed scheme. Section IV shows experimental results and Section V discusses the impact and meaning of the results. Section VI then draws relevant conclusions.

II. Voltage-Constrained Energy-Harvesting Scheme

The proposed voltage-constrained energy-harvesting system features a battery that both clamps the variable capacitor voltage and stores the harvested energy [45]. The process operates in three separate steps, as illustrated in Figure 2. First, the battery invests an initial amount of energy to pre-charge the capacitor to the battery voltage when its capacitance is highest (C_{MAX}). This investment constitutes an energy loss in the system, which assuming no other losses exist in the transfer, is

$$\Delta E_{Invested} \equiv E_{CAP} = \tfrac{1}{2}C_{MAX}V_{BAT}^2. \quad (2)$$

Mechanical forces from ambient vibrations then work against the capacitor's established electrostatic force and cause capacitance C_{VAR} to decrease, converting mechanical energy to electrical in the process. The converted mechanical energy plus the electrical energy removed from the capacitor (as charge is driven out of C_{VAR}) charge the battery in the form of i_{HARV}, which now produces a harvest of

$$\Delta E_{Harvested} = \int V_{BAT} i_{HARV}(t)dt = V_{BAT}^2 \int \frac{dC(t)}{dt}dt = V_{BAT}^2 \Delta C. \quad (3)$$

Ideally, once minimum capacitance C_{MIN} is reached, the same pre-charge block transfers the energy that remains back to the battery, effectively resulting in another gain of

$$\Delta E_{Recovered} = \tfrac{1}{2}C_{MIN}V_{BAT}^2 \quad (4)$$

and yielding a net gain for the system of

$$\Delta E_{NET} = \Delta E_{Harvested} + \Delta E_{Recovered} - \Delta E_{Invested} = \tfrac{1}{2}\Delta C V_{BAT}^2. \quad (5)$$

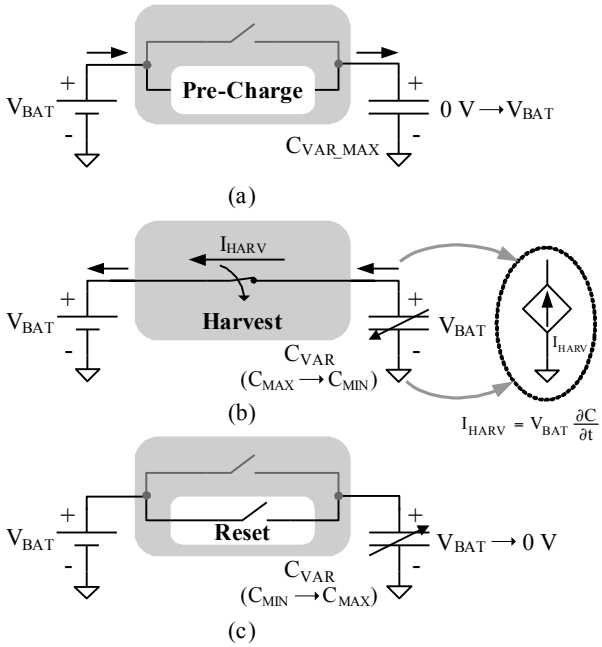

Figure 2. Voltage-constrained energy-harvesting steps: (a) pre-charge, (b) harvest, and (c) reset.

The process of transferring energy, however, is not lossless and the system therefore loses some energy in all three steps, which is one of the fundamental challenges of harvesters. In fact, if the energy available for recovery ($\Delta E_{Recovered}$) is less than the energy losses incurred during the recovery process, it is more efficient to omit the step altogether, as in the foregoing system. To be more specific, after harvesting, C_{VAR} is left open circuited, in other words, under charge-constrained

conditions. As a result, as vibrations force C_{VAR} to increase again, its voltage naturally resets (i.e., decreases) to a substantially lower voltage (near zero), that is, to V_{BAT} times minimum-maximum capacitance ratio C_{MIN}/C_{MAX}. Nevertheless, the energy harvested still exceeds the investment, leaving a theoretical gain of

$$\Delta E_{NET} = \left(\tfrac{1}{2}C_{MAX} - C_{MIN}\right)V_{BAT}^2, \quad (6)$$

where energy-transfer losses account for lower ΔE_{NET} values.

III. Proposed Energy-Harvesting System

A. Topology

Since inductors are quasi-lossless devices, to maximize energy gain, an inductor-based pre-charger that transfers energy from the battery to variable capacitor C_{VAR}, as seen in Figure 3, is implemented. Inductor L is first energized by imposing battery voltage V_{BAT} across it with switches S_1 and S_3. Inductor current i_L consequently increases linearly until sufficient energy is stored, at which point switches S_1 and S_3 open and S_2 and S_4 close and channel the stored energy to C_{VAR}. This pre-charge step occurs at maximum capacitance, just before the onset of the harvesting phase.

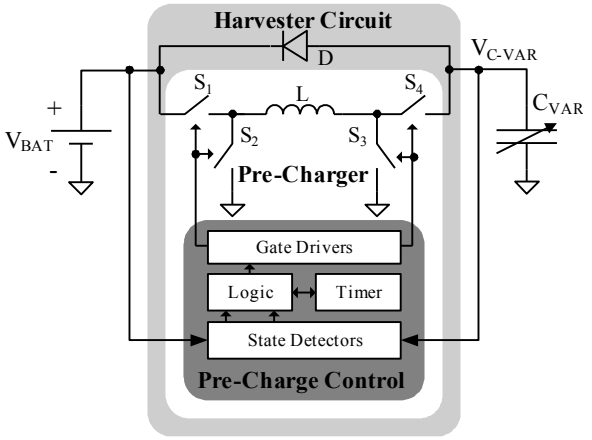

Figure 3. Proposed energy-harvesting and battery-charging system.

Once C_{VAR} is pre-charged, as capacitance decreases, battery V_{BAT} clamps capacitor voltage $V_{C\text{-}VAR}$ via either a synchronous switch or an asynchronous diode and the resulting harvesting current charges the battery. Note that, while a synchronous switch may dissipate lower Ohmic losses (because the voltage across its terminals is low), the energy used in the additional circuitry required to synchronize it (i.e., prevent reverse current flow) offsets some, if not all, of those gains. A diode, on the other hand, naturally conducts current only in one direction (towards the battery) so it only dissipates Ohmic losses, which given the current levels, are substantially low to begin with. As a result, considering the power, risk, and complexity associated with the synchronous switch, the asynchronous diode offers a more appealing proposition.

The pre-charge control block illustrated in Figure 3 senses when to pre-charge C_{VAR} (at maximum capacitance) and applies the proper gate-drive signal configuration for a pre-determined inductor-energizing time ($\Delta t_{PRE\text{-}CHARGE}$). To determine when to pre-charge C_{VAR}, instead of sensing capacitance directly, which might require ac currents or voltages, the pre-charger detects when capacitance reaches C_{MAX} and starts to decrease by monitoring the capacitor voltage $V_{C\text{-}VAR}$. Since C_{VAR} is charge constrained (i.e., open circuit: $C_{VAR} = Q_{CONSTANT}/V_{C\text{-}VAR}$) during its reset phase, $V_{C\text{-}VAR}$ increases as soon as C_{VAR} starts to decreases from its maximum value of C_{MAX}. At this point, if $V_{C\text{-}VAR}$ is less than V_{BAT}, pre-charge commences, and because the pre-charge time is on the order of nanoseconds and therefore substantially shorter than the vibration period, which is in milliseconds, capacitance remains close to its maximum value. Note that detecting the state of C_{VAR} also conveys motion information so the system can also double as a vibration sensor.

Pre-charge time $\Delta t_{PRE\text{-}CHARGE}$ is preset to energize the inductor with sufficient energy to subsequently charge the capacitor to V_{BAT}. During this time, inductor current i_L increases linearly to a maximum value of

$$I_{L(max)} = \frac{V_{BAT}}{L}\Delta t_{PRE-CHARGE}. \quad (7)$$

As a result, the amount of energy transferred to inductor L is

$$E_L = \tfrac{1}{2}LI_{L(max)}^2 = \frac{1}{2L}\left(V_{BAT}\Delta t_{PRE-CHARGE}\right)^2, \quad (8)$$

and equating this to the invested energy required to pre-charge C_{VAR} (E_{CAP} or $\Delta E_{Invested}$), as derived in (2), yields a pre-charge time of

$$E_L = E_{CAP} \rightarrow \Delta t_{PRE-CHARGE} = \sqrt{LC_{MAX}}, \quad (9)$$

which is independent of V_{BAT}, assuming quasi-lossless energy transfers. Consequently, even as V_{BAT} changes (Li Ion spans 2.7-4.2 V across its state of charge), a constant $\Delta t_{PRE\text{-}CHARGE}$ transfers sufficient energy to C_{VAR}. In practice, $\Delta t_{PRE\text{-}CHARGE}$ is set slightly higher to offset the energy losses associated with the transfer.

Pre-charge ends as soon as capacitor voltage $V_{C\text{-}VAR}$ equals or surpasses battery voltage V_{BAT}, when all switches turn OFF. Excess energy in the inductor returns to the battery through the harvesting diode by charging C_{VAR} a diode voltage above V_{BAT} and subsequently transferring the remainder through the now forward-biased diode. It is best to minimize this extra energy to reduce the losses associated with transferring energy through the system.

B. Circuitry

The proposed energy-harvesting power-train circuit, which is comprised of the harvesting diode and pre-charge CMOS switches MP_1, MN_2, MN_3, and transmission gate MN_4-MP_4, as illustrated in Figure 4, was fabricated with the 1.5 µm CMOS process technology available from AMI Semiconductor foundry [46]. The control electronics were kept off chip for experimental flexibility and ease of reach.

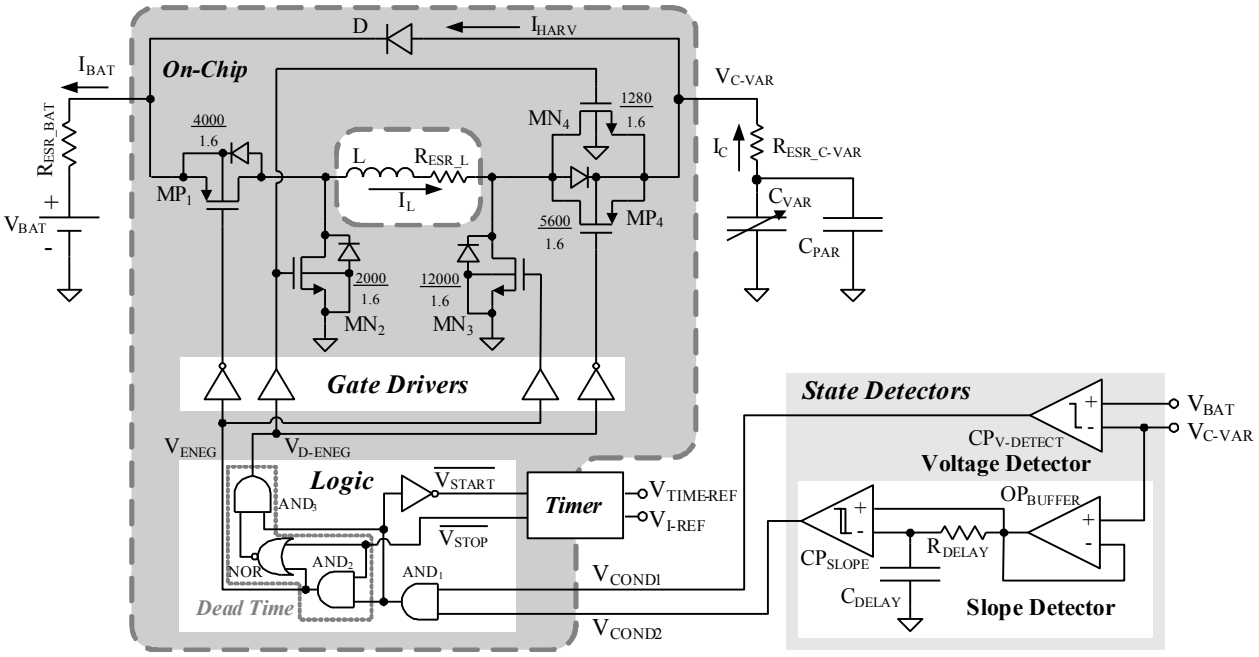

Figure 4. Complete energy-harvesting and battery-charging system prototype implementation (dimensions in μm).

The system energizes inductor L when transistors MP_1 and MN_3 are ON, and subsequently channels the stored energy to variable capacitor C_{VAR} when MN_2 and transmission gate MP_4-MN_4 conduct, after MP_1 and MN_3 are OFF. Complementary switches MP_4-MN_4 realize switch S_4 because MP_4 alone lacks gate drive to conduct enough current when the capacitor is initially discharged. Individual on-chip buffers drive each power switch, except for MN_4, which shares its driving signal with MN_2. The harvesting diode connecting the capacitor to the battery is a diode-connected NPN transistor - AMI's 1.5 μm CMOS technology offers vertical n-type BJTs.

To detect the state of C_{VAR}, and thus determine when to pre-charge it, an off-chip control circuit is used. Comparator $CP_{V\text{-}DETECT}$ detects the first condition required to start the pre-charge process, which is to ascertain when $V_{C\text{-}VAR}$ falls below V_{BAT}. The propagation delay of this comparator should be sufficiently short to ensure the pre-charge phase stops before C_{VAR} charges above its target value (V_{BAT}), which could otherwise incur additional losses in the system. Slope detecting comparator CP_{SLOPE} detects whether or not the second condition is met, that $V_{C\text{-}VAR}$ rises (when C_{VAR} starts to decrease from its maximum value of C_{MAX}), by comparing $V_{C\text{-}VAR}$ with its previous state ($V_{C\text{-}DELAY}$), a delayed version of itself. That way, if $V_{C\text{-}VAR}$ increases (or decreases), $V_{C\text{-}DELAY}$ is lower (or higher) and CP_{SLOPE} therefore asserts an enabling (or disabling) signal. A 5 MΩ and 4.7 nF RC circuit implements a delay of approximately 20 ms and buffer OP_{BUFFER} isolates and decouples C_{VAR} from the RC circuit. The comparators include some hysteresis to desensitize the circuit to glitches and any other extraneous noise present.

When the aforementioned conditions are met, on-chip logic controls the pre-charge switching sequence, including dead time between oppositely phased digital signals to avoid transient shoot-through (short-circuit) power losses in the pre-charger switches. Logic gate AND_1 enables a timer with signal $\overline{V_{START}}$ and starts the energizing process of inductor L via signal V_{ENEG}, while $V_{D\text{-}ENEG}$ is low.

After the timer reaches its preset value, it flags the logic to stop energizing L with signal $\overline{V_{STOP}}$, which forces V_{ENEG} to drop and, after a dead-time delay, prompts the circuit to de-energize L via $V_{D\text{-}ENEG}$, when it goes high (all switches are OFF during dead time). The combined propagation delay of gates AND_2, AND_3, and NOR determines this dead time. The de-energizing switches remain ON until the first condition is no longer true, when $V_{C\text{-}VAR}$ is again greater than V_{BAT}, at which point the logic disables the timer and shuts off all MOS switches.

The energizing time of the inductor is set with the timer circuit shown in Figure 5. Once reset and enabled by the logic block (i.e., MN_{RESET} is turned OFF), the circuit triggers a cut-off signal when comparator CP_{TIMER} senses that linearly increasing ramp voltage V_{RAMP} surpasses pre-set reference voltage $V_{TIME\text{-}REF}$, the latter of which effectively sets the total energizing time for the inductor. Charging on-chip capacitor C_{RAMP} with a constant current-source reference produces V_{RAMP}. The current source is realized by forcing reference voltage $V_{I\text{-}REF}$ across resistance $R_{I\text{-}REF}$ via the negative feedback loop comprised of op-amp $OP_{I\text{-}REF}$ and transistor $MN_{I\text{-}REF}$. This reference current is subsequently mirrored and amplified by a factor of five (i.e., N = 5) before channeling it to C_{RAMP}:

$$I_{RAMP} = N\left(\frac{V_{I-REF}}{R_{I-REF}}\right), \tag{10}$$

linearly charging C_{RAMP} with a slope of

$$\left(\frac{\Delta V}{\Delta t}\right)_{RAMP} = \frac{I_{RAMP}}{C_{RAMP}} \quad (11)$$

and defining $V_{TIME\text{-}REF}$ to

$$V_{TIME-REF} = \Delta t_{PRE-CHARGE}\left(\frac{\Delta V}{\Delta t}\right)_{RAMP}. \quad (12)$$

In practice, parasitic capacitors in parallel to C_{RAMP} slow the rising ramp rate so $V_{TIME\text{-}REF}$ should be lower.

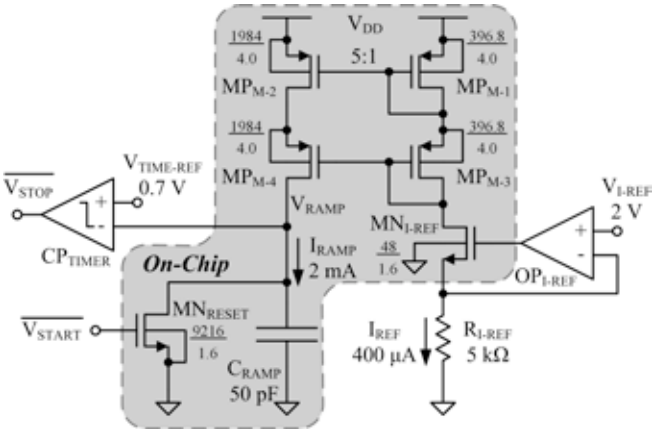

Figure 5. Energizing timer-circuit schematic (dimensions in µm).

IV. Experimental Results and Evaluation

The power switches, gate drivers, digital logic, diode, and part of the timer were fabricated on 1.4 mm x 1.8 mm of the 2.2 mm x 2.2 mm die shown in Figure 6 using AMI's 1.5 µm CMOS process. A 3 V supply emulated a moderately charged Li Ion (V_{BAT}), whose full range normally spans 2.7 to 4.2 V. The off-chip surface-mount 4 mm x 4 mm x 2 mm inductor package used had an inductance of roughly 10.72 µH with an equivalent series resistance (ESR) of 240 mΩ. Manually turning a trimmer capacitor with a maximum-minimum capacitance range of approximately 250 to 60 pF, including parasitic capacitances present (measured), emulated the harvesting device under vibration conditions. Although continually turning the manual capacitor to charge a battery would have been ideal, the process was impractical because of its non-periodic nature and the human element of fatigue; however, the objective of the set-up was to test the viability of the harvesting scheme on a per cycle basis, not its steady-state behavior, which is the subject of further research.

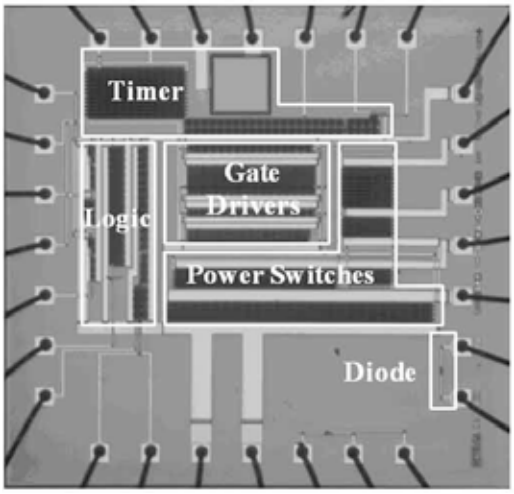

Figure 6. Die photograph of the 2.2 mm x 2.2 mm 1.5 µm CMOS energy-harvesting and battery-charging system prototype.

A. Harvest with Direct Pre-Charge

To prove harvesting is possible by constraining voltage, the capacitor is manually pre-charged and decreased. Momentarily shorting the variable capacitor to the supply after setting it to its maximum capacitance, manually pre-charges (i.e., prepares) the device. The capacitor is subsequently decreased manually and its resulting current recorded. Turning the capacitor, however, is a manual process and the device's response is consequently nonlinear, introducing what appears to be noise. The finite delay between the initialization process and actually turning the device further introduces inaccuracies, allowing parasitic drain currents to discharge the capacitor slightly from its initial value. Nonetheless, Figure 7 shows the harvesting currents the variable capacitor drive through the diode to the battery supply for two different sets of measurements. Integrating the power harvested, which is the product of the measured current and battery voltage V_{BAT}, over the cycle time yielded 6.11 and 6.37 nJ for the results shown and an average of 5.82 nJ across eight separate measurements.

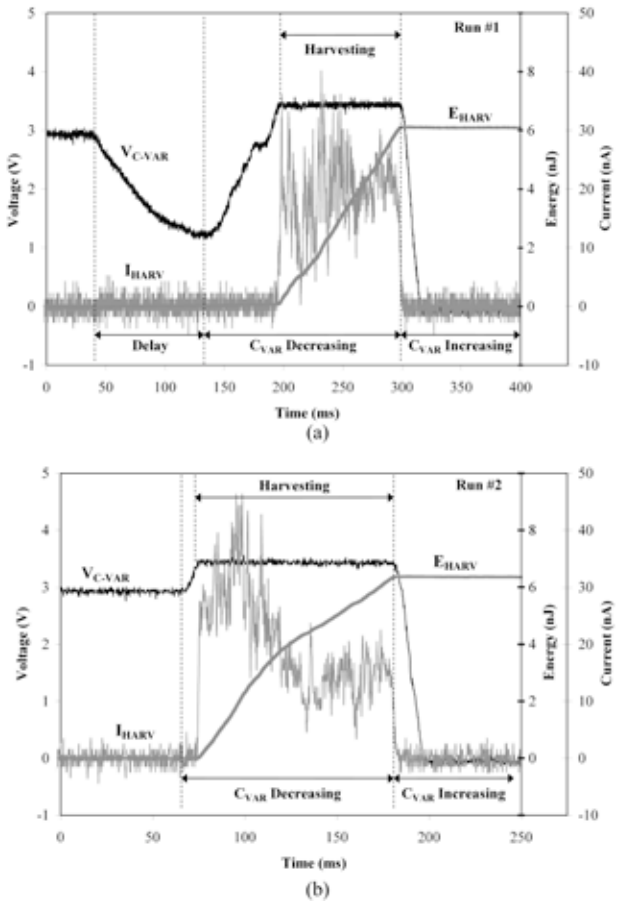

Figure 7. (a)-(b) Sample harvest measurements by directly pre-charging variable capacitor C_{VAR}.

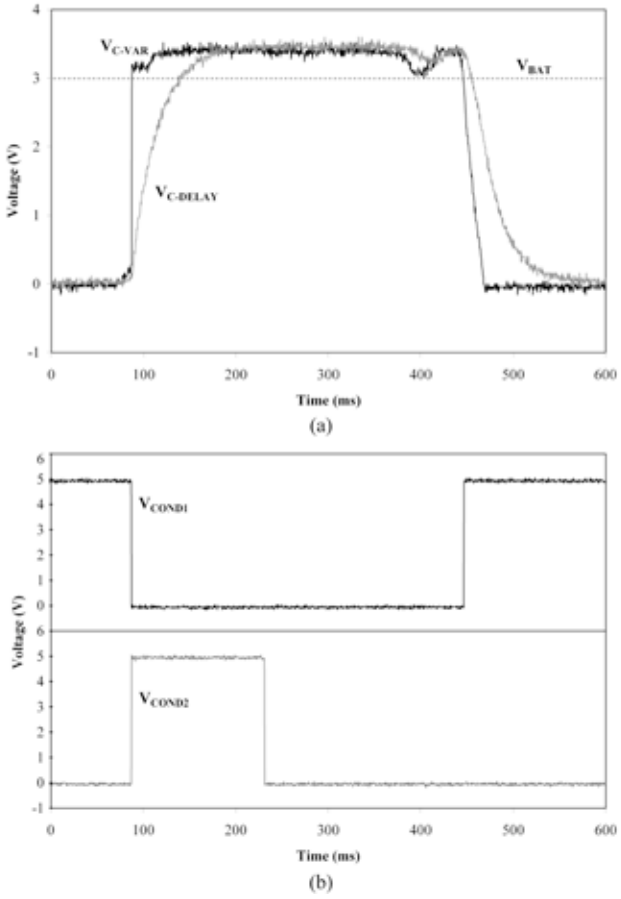

Figure 8. Detection of pre-charge conditions: (a) variable capacitor voltage $V_{C\text{-}VAR}$ increases (its delayed version $V_{C\text{-}DELAY}$ is lower) and (b) the state detector outputs V_{COND1} and V_{COND2}.

B. Pre-Charge

The pre-charger was then tested by allowing the system to (1) detect the conditions necessary for a pre-charge cycle, (2) initiate the sequence, and (3) charge variable capacitor C_{VAR} to battery voltage V_{BAT}. To this end, C_{VAR} was set at its maximum capacitance point and turned. Figure 8 shows how both conditions for pre-charge are detected. First, during the reset phase, before pre-charge, V_{COND1} is high because $V_{C\text{-}VAR}$ is less than or equal to V_{BAT}. As soon as $V_{C\text{-}VAR}$ begins to increase, which indicates that C_{VAR} (under charge-constrained conditions) starts to decrease from its maximum value of C_{MAX}, V_{COND2} switches to a high state because $V_{C\text{-}VAR}$ exceeds its delayed version $V_{C\text{-}DELAY}$, which means the pre-charge sequence initiates.

Figure 9(a) shows control signals V_{ENEG} and $V_{D\text{-}ENEG}$ when subjected to this test, the former of which instructs the system to energize inductor L and the latter to release its stored energy to C_{VAR}. As L is energized, V_{BAT} (3 V) is impressed across L (inductor voltage V_L is shown in Figure 9(b)), forcing an inductor current of 17.61 mA (on average) and resulting in an average invested energy per cycle of 1.66 nJ. This energy level is greater than what is required by C_{VAR} because it includes transfer losses that must be surmounted, as analyzed and derived in [45]. When de-energizing L, V_L is reversed by connecting L to C_{VAR}, gradually releasing energy to C_{VAR} and consequently increasing its voltage $V_{C\text{-}VAR}$.

While MN_2's drain capacitance is completely drained at the end of pre-charge, just after all switches turn off, remnant (excess) energy in L and MN_3's charged drain capacitance shifts back and forth (i.e., resonates) between L and both drain capacitances. LC oscillations therefore result until parasitic resistances present eventually dampen them completely. This excess energy represents an over-investment on the part of the pre-charge circuit. For context, consider that 10 pF of parasitic capacitance produces the oscillations measured when 45 pJ of excess energy is available at 3 V, which means excess energy constitutes only a small fraction of the average invested energy of 1.66 nJ/cycle.

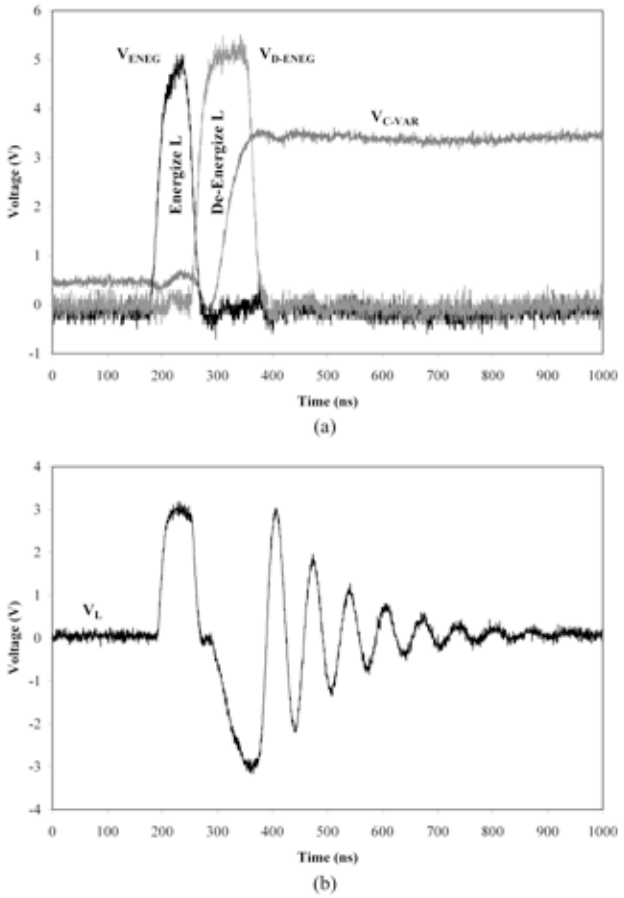

Figure 9. Pre-charge waveforms: (a) inductor energizing and de-energizing control signals V_{ENEG} and $V_{D\text{-}ENEG}$ with corresponding variable capacitor voltage $V_{C\text{-}VAR}$ and (b) inductor voltage V_L.

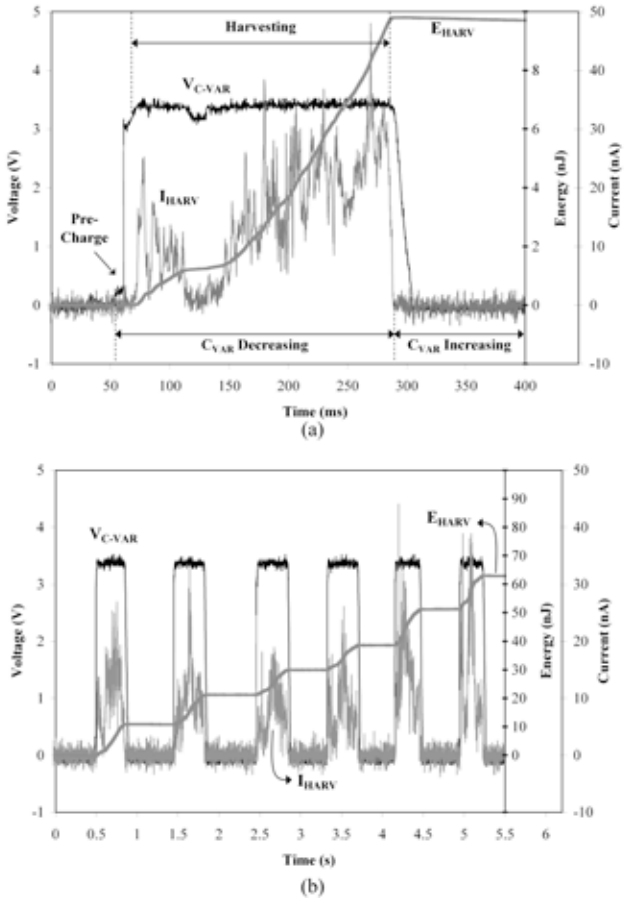

Fig. 10. System-level measurements showing variable capacitor C_{VAR} voltage $V_{C\text{-}VAR}$, harvesting current I_{HARV}, and extrapolated energy profile E_{HARV} during (a) one complete and (b) six maximum-minimum-maximum C_{VAR} cycles.

C. System Test: Pre-Charge and Harvest

After determining the pre-charger was functional, full system-level experiments were performed, verifying pre-charge and harvest automatically cycled with variations in C_{VAR}, as designed and shown experimentally in Figure 10. The average energy per cycle directed to the battery over 126 different sets of measurements was 9.7 nJ/cycle (Figure 10(a) is a sample run), giving a net energy gain, E_{GAIN}, (by subtracting the investment from the harvest) of approximately 8 nJ/cycle. Figure 10(b) illustrates the results of continually turning the trim capacitor for six consecutive cycles, harvesting a total of 63 nJ over the span of the six cycles shown (not subtracting the corresponding investment energy).

V. Discussion

A few comments on the results are worth mentioning at this point. (1) Because there is no manual (i.e., artificial) delay between the pre-charge phase and capacitor C_{VAR} decreasing, more average energy per cycle is harvested than under the direct (i.e., manual) pre-charge method. (2) Average power in these measurements depends on the vibration frequency (cycles per second f_{VIB}) of the system and the mechanical design of the variable capacitor ($P_{GAIN} = E_{GAIN}f_{VIB}$). Considering many applications exhibit accelerations in the 1-500 Hz frequency range, such as a person tapping their heels at 1 Hz and a car engine vibrating at 200 Hz [20], the proposed system, when subjected to vibrations of 200 Hz, could gain 1.6 µJ every second, that is, 1.6 µW of average power. (3) Manually turning the trimming capacitor is considerably slower than 200 Hz, demanding an impractically large $R_{DELAY}C_{DELAY}$ delay that dissipates more energy than in actual applications. So for instance, 12.5 pF and 20 MΩ would yield a delay nearing 250 µs (i.e., 5 % of the total 200 Hz cycle) and require only about 112.5 pJ/cycle. (4) Gate drivers and controller circuit must be optimized for low energy.

Gate-Drive and Controller Losses: Since parts of the pre-charger could not be optimized for low energy because their physical parameters (such as transistor aspect ratios and circuit configuration) were pre-set, they were powered from a separate supply (V_{DD}) so that unreasonable power requirements would not otherwise mislead the experimental results obtained. Understanding the impact these requirements have on the energy harvested, however, is nonetheless important. To this end, multiplying the gate-oxide capacitance per unit area (C_{OX}) of the process (e.g., 1.12 fF/µm^2) by the total gate area of the power switches (Figure 4) indicates gate-drive losses from a 3 V supply are approximately 401.3

pJ/cycle. Similarly, three- and four-stage gate drivers require roughly 266 pJ/cycle to drive all power transistors. Collectively, gate-drive and driver losses sum to 667.3 pJ/cycle, which means the projected net energy gain of the harvester reduces from 8 to 7.33 nJ/cycle.

Reducing the controller's quiescent energy to pJ levels per cycle is possible by resizing and biasing transistors to operate in subthreshold (given high-speed circuits are not necessary to process low vibration frequencies) and leveraging and duty-cycling already-existing circuit blocks (i.e., operate components only for short spurts and duel them for other functions). Comparators $CP_{V\text{-}DETECT}$ and CP_{SLOPE} (Figure 4), for one, can be biased with 5 nA each, dissipating about 150 pJ/cycle at 200 Hz cycles. Pre-charge, for another, occurs only within a small fraction of the entire cycle (e.g., 200 ns of the 5 ms period, assuming a vibration frequency of 200 Hz) so the components used to control it can be disabled during the remainder of the period (e.g., off for 4.9998 ms of 5 ms). Biasing comparator CP_{TIMER} and amplifier $OP_{I\text{-}REF}$ with 25 μA each from a 3 V supply only draws 30 pJ/cycle when operating for 200 ns of the 5 ms period. The 2.4 mA that flows into the timer circuit (Figure 5) would dissipate about 1.44 nJ/cycle when limited to 200 ns of the 5 ms period. More importantly, however, further reducing its energy is possible by decreasing C_{RAMP} to, say, 5 pF and its charging current I_{RAMP} to 200 μA, reducing 2.4 mA and 1.44nJ/cycle to 240 μA and 144 pJ/cycle. In the end, when considering all measured and projected power losses, the proposed converter's net energy gain can be 6.9 nJ/cycle at 200 Hz.

Battery: The battery's equivalent series resistance (ESR) also dissipates conduction power during pre-charge. Just to cite an example, a commercially available Li-Ion polymer battery (from PowerStream PGE014461) offers 200 mAh of capacity with an ESR of 180 mΩ, which is on the same order as the inductor's ESR [47] and therefore its impact on efficiency is, for all practical purposes, negligible. The only other possible loss associated with the battery can be the electronics used to monitor the Li Ion's state of charge during the charging process. Fortunately, most of the circuit can be disabled, except for a slow and relatively inaccurate voltage detector whose purpose is to engage the rest of the circuit when the Li Ion voltage is near 4 V. In other words, efficiency remains unchanged and decreases only when the battery is near its fully charged state, at which point the system's need for energy is less acute.

Voltage-Constrained Harvesters: Unlike in charge-constrained schemes, voltage-constraining harvesting capacitor C_{VAR} protects the circuit from voltages that exceed the breakdown limits of standard CMOS technologies [37]-[38]. Additionally, voltage-constraining C_{VAR} with the already-existing battery that is to be charged enhances integration because no additional source is required. One drawback is that the energy harvested is proportional to the battery's voltage, which means less energy is harvested at lower battery voltages. What is more, preferably, the constraining voltage should vary to match the harvesting electrostatic force with other mechanical damping forces to achieve optimum energy conversion from vibrations [19]-[20]. The pre-charger and control circuitry could viably boost this voltage up to the maximum allowed process voltage, regardless of battery conditions, except doing so increases complexity and controller losses.

Summary: The purpose of this paper (and contribution) is to show experimentally the proposed prototyped circuit is able to draw energy from a variable voltage-constrained capacitor. Although the controller and switches were not optimized in their present form for power efficiency because functionality was more important, projections show that a net energy gain (after considering *all* losses) is possible. Note an important feature (and contribution) of the proposed solution is also its ability to automatically detect when to pre-charge the capacitor without having to sense or measure capacitance, or accurately synchronize the system to capacitor variations. Finally, as mentioned earlier in the paper, given the innate nature of the harvester, the presented prototype also doubles as a vibration sensor, increasing the functional efficiency and the packing density of the final solution.

VI. Conclusions

The prototyped circuit (which pre-charges, detects, and synchronizes to a variable voltage-constrained capacitor) and accompanying experimental results presented show that the proposed energy-scavenging, battery-charging system harvests 9.7 nJ per cycle from a 200 pF capacitance variation, in other words, that harvesting energy electrostatically from vibrations is possible. The solution requires an investment of 1.7 nJ/cycle and results in a net energy gain of approximately 8 nJ/cycle with 1.6 μW at 200 Hz, excluding gate-drive or control-circuit losses (portions of which could not be optimized because they were pre-set). Projecting and including practical values for these latter losses, reduces the net energy gain to 6.9 nJ/cycle.

The underlying feature of the proposed system is using the battery receiving the energy as both the voltage-constraining device and pre-charge source. The driving technology is the circuit, which allows the variable capacitor to drive charge back to the battery when capacitance decreases, effectively synchronizing the circuit to the capacitance variations that result in response to ambient vibrations. These results prove that the mechanical energy in vibrations, which are naturally abundant in many practical applications, can be scavenged and channeled to a rechargeable energy-storage device (e.g., a battery). By applying low-power and duty-cycling techniques to the loading system so that it demands low power, the harvested energy can viably replenish the total energy consumed by the system, potentially extending its operational life indefinitely without manual/external re-charge or battery-replacement cycles, which may be otherwise prohibitive in applications like remote wireless micro-sensors and bio-implantable devices.

VII. Acknowledgement

The authors would like to thank Texas Instruments for their sponsorship and support of this research.

REFERENCES

[1] D. Puccinelli and M. Haenggi, "Wireless sensor networks: applications and challenges of ubiquitous sensing," *IEEE Circuits and Systems Magazine*, vol. 3, no. 3, pp. 19-29, 2005.

[2] P. Dario, M.C. Carrozza, A. Benvenuto, and A. Menciassi, "Micro-systems in biomedical applications," *Journal of Micromechanics and Microengineering*, vol. 10, no. 2, pp. 235-244, June 2000.

[3] A. Shamim, M. Arsalan, L. Roy, M. Shams, and G. Tarr, "Wireless dosimeter: system-on-chip versus system-in-package for biomedical and space applications," *IEEE Transactions on Circuits and Systems II*, vol. 55, no. 7, pp. 643-647, July 2008.

[4] P. Li and R. Bashirullah, "A wireless power interface for rechargeable battery operated medical implants," *IEEE Transactions on Circuits and Systems II*, vol. 54, no. 10, pp. 912-916, Oct. 2007.

[5] J.P. Vogt and Rincón-Mora, "SiP wireless micro-power sensors," presented at *Government Microcircuit Applications and Critical Technology Conference*, Lake Buena Vista, FL, 2007.

[6] N.G. Elvin, N. Lajnef, and A.A. Elvin, "Feasibility of structural monitoring with vibration powered sensors," *Smart Materials and Structures*, vol. 15, no. 4, pp. 977-986, Aug. 2006.

[7] J.B. Bates, N.J. Dudney, B. Neudecker, A. Ueda, and C.D. Evans, "Thin-film lithium and lithium-ion batteries," *Solid State Ionics*, vol. 135, pp. 33-45, Nov. 2000.

[8] W. Mustain, S. Prakash, H. Kim, P. Kohl, and G.A. Rincón-Mora, "Micro DMFC – lithium ion hybrid power source for low power applications," *Proc. 212th Meeting of the Electrochemical Society*, 2007.

[9] E.O. Torres and G.A. Rincón-Mora, "Long-lasting, self-sustaining, and energy-harvesting system-in-package (SiP) wireless micro-sensor solution," *Proc. International Conference on Energy, Environment, and Disasters (INCEED)*, 2005.

[10] S. Roundy, D. Steingart, L. Frechette, P. Wright, and J. Rabaey, "Power sources for wireless sensor networks," *Proc. 1st European Wireless Sensor Networks Workshop*, pp. 1-17, 2004.

[11] S. Roundy, P.K. Wright, and J.M. Rabaey, *Energy Scavenging for Wireless Sensor Networks with Special Focus on Vibrations*, 1st ed., Massachusetts: Kluwer Academic Publishers, 2004.

[12] L. Collins, "Harvest for the world" *IEE Power Engineer*, vol. 20, no. 1, pp. 34-37, Feb. 2006.

[13] B.A. Warneke, M.D. Scott, B.S. Leibowitz, L. Zhou, C.L. Bellew, J.A. Chediak, J.M. Kahn, B.E. Boser, and K.S. Pister, "An autonomous 16 mm^3 solar-powered node for distributed wireless sensor networks," *Proc. of IEEE Sensors*, vol. 1, no. 2, pp. 1510-1515, 2002.

[14] C. Alippi and C. Galperti, "An adaptive system for optimal solar energy harvesting in wireless sensor network nodes," *IEEE Transactions on Circuits and Systems I*, vol. 55, no. 6, pp. 1742-1750, July 2008.

[15] M. Stordeur and I. Stark, "Low power thermoelectric generator – self-sufficient energy supply for micro systems," *Proc. 16th International Conference on Thermoelectrics*, pp. 575-577, 1997.

[16] H.A. Sodano, G.E. Simmers, R. Dereux, and D. Inman, "Recharging batteries using energy harvested from thermal gradients," *Journal of Intelligent Material Systems and Structures*, vol. 18, no. 1, pp. 3-10, Jan. 2007.

[17] W. Wang, F. Jia, Q. Huang, and J. Zhang, "A new type of low power thermoelectric micro-generator fabricated by nanowire array thermoelectric material," *Microelectronic Engineering*, vol. 77, no. 3-4, pp. 223-229, Apr. 2005.

[18] C.B. Williams and R.B. Yates, "Analysis of a micro-electric generator for microsystems," *Sensors and Actuators A*, vol. 52, no. 1-3, pp. 8-11, Mar.-Apr. 1996.

[19] S.P. Beeby, M.J. Tudor, and N.M. White, "Energy harvesting vibration sources for microsystems applications," *Measurement Science and Technology*, vol. 17, no. 12, pp. R175-195, Dec. 2006.

[20] S. Roundy, P. Wright, and J. Rabaey, "A study of low level vibrations as a power source for wireless sensor nodes," *Computer Communications*, vol. 26, no. 11, pp. 1131-44, July 2003.

[21] P.D. Mitcheson, T.C. Green, E.M. Yeatman, and A.S. Holmes, "Architectures for vibration-driven micropower generators," *IEEE Journal of Microelectromechanical Systems (MEMS)*, vol. 13, no. 3, pp. 429-440, June 2004.

[22] S.P. Beeby, R.N. Torah, M.J. Tudor, P. Glynne-Jones, T. O'Donnell, C.R. Saha, and S. Roy, "A micro electromagnetic generator for vibration energy harvesting," *Journal of Micromechanics and Microengineering*, vol. 17, pp. 1257-1265, July 2007

[23] H. Kulah and K. Najafi, "An electromagnetic micro power generator for low-frequency environmental vibrations," *Proc. 17th IEEE Conference on Micro Electro Mechanical Systems (MEMS)*, pp. 237-240, 2004.

[24] M. El-Hami, P. Glynne-Jones, N.M. White, M. Hill, S. Beeby, E. James, A.D. Brown, and J.N. Ross, "Design and fabrication of a new vibration-based electromechanical power generator," *Sensors and Actuators A*, vol. 92, no. 1-3, pp. 335-342, Aug. 2001.

[25] R. Amirtharajah and A.P. Chandrakasan, "Self-powered signal processing using vibration-based power generation," *IEEE Journal of Solid-State Circuits*, vol. 33, no. 5, pp.687-695, May 1998.

[26] S. Yuen, J. Lee, W.J. Li, and P. Leong, "An AA-sized vibration-based microgenerator for wireless sensors," *Pervasive Computing*, vol. 6, no. 1, pp. 64-72, Jan. Mar. 2007.

[27] S. Meninger, J. Mur-Miranda, R. Amirtharajah, A. Chandrakasan, and J Lang, "Vibration-to-electric energy conversion," *IEEE Transactions on Very Large Scale Integration (VLSI) Systems*, vol. 9, no. 1, pp. 64-76, Feb. 2001.

[28] S. Roundy, P.K. Wright, and K.S.J. Pister "Micro-electrostatic vibration-to-electricity converters" *Proc. ASME International Mechanical Engineering Congress and Exposition*, pp. 1-10, 2002.

[29] E. Lefeuvre, A. Badel, C. Richard, L. Petit, and D. Guyomar, "A comparison between several vibration-powered piezoelectric generators for standalone systems," *Sensors and Actuators A*, vol. 126, no. 2, pp.405-416, Feb. 2006.

[30] H.A. Sodano, D.J. Inman, and G. Park, "Generation and storage of electricity from power harvesting devices," *Journal of Intelligent Material Systems and Structures*, vol. 16, no. 1, pp. 67-75, Jan. 2005.

[31] S. Roundy and P.K. Wright, "A piezoelectric vibration based generator for wireless electronics," *Smart Materials and Structures*, vol. 13, no. 5, pp. 1131-1142, Oct. 2004.

[32] G.K. Ottman, H.F. Hofmann, and G.A. Lesieutre, "Optimized piezoelectric energy harvesting circuit using step-down converter in discontinuous conduction mode," *IEEE Transactions on Power Electronics*, vol. 18, no. 2, pp. 696-703, Mar. 2003.

[33] X. Wang, J. Song, J. Liu, and Z.L. Wang, "Direct-Current nanogenerator driven by ultrasonic waves," *Science*, vol. 316, no. 5821, pp. 102-105, Apr. 2007.

[34] S. Xu, K.D.T. Ngo, T. Nishida, G.B. Chung, and A. Sharma, "Low frequency pulsed resonant converter for energy harvesting," *IEEE Transactions on Power Electronics*, vol. 22, no. 1, pp. 63-68, Jan. 2007.

[35] P.D. Mitcheson, P. Miao, B.H. Stark, E.M. Yeatman, A.S. Holmes, and T.C. Green, "MEMS electrostatic micropower generator for low frequency operation," *Sensors and Actuators A*, vol. 115, no. 2-3, pp. 523-529, Sept. 2004.

[36] G. Despesse, T. Jager, J.J. Chaillout, J.M. Leger, and S. Basrour, "Design and fabrication of a new system for vibration energy harvesting," *Proc. PhD. Research in Microelectronics and Electronics*, vol. 1, pp. 225-228, 2005.

[37] B.H. Stark, P.D. Mitcheson, P. Miao, T.C. Green, E.M. Yeatman, and A.S. Holmes, "Converter circuit design, semiconductor device selection and analysis of parasitics for micropower electrostatic generators," *IEEE Transactions on Power Electronics*, vol. 21, no. 1, pp. 27-37, Jan. 2006.

[38] B.H. Stark and T.C. Green "Comparison of SOI power device structures in power converters for high-voltage, low-charge electrostatic microgenerators," *IEEE Transactions on Electron Devices*, vol. 52, no. 7, pp. 1640-1648, July 2005.

[39] T. Sterken, P. Fiorini, K. Baert, R. Puers, and G. Borghs, "An electret-based electrostatic μ-generator," *Proc. 12th International Conference on Solid State Sensors, Actuators, and Microsystems*, pp. 1291-1294, 2003.

[40] T. Sterken, K. Baert, R. Puers, G. Borghs, and R. Mertens, "A new power MEMS component with variable capacitance," *Proc. Pan-Pacific Microelectronics Symposium*, pp. 27-34, 2003.

[41] F. Peano and T. Tambosso, "Design and optimization of a MEMS electret-based capacitive energy scavenger," *IEEE Journal of Microelectromechanical Systems (MEMS)*, vol. 14, no. 3, June 2005.

[42] W. Ma, R. Zhu, L. Rufer, Y. Zhohar, and M. Wong, "An integrated floating-electrode electric microgenerator," *IEEE Journal of Microelectromechanical Systems (MEMS)*, vol. 16, no. 1, Feb. 2007.

[43] R. Tashiro, N. Kabei, K. Katayama, Y. Ishizuka, F. Tsuboi, and K. Tsuchiya, "Development of an electrostatic generator that harnesses the motion of a living body," *JSME International Journal, Series C: Mechanical Systems, Machine Elements and Manufacturing*, vol .43, no. 4, pp. 916-922, Dec. 2000.

[44] B.C. Yen and J.H. Lang, "A variable-capacitance vibration-to-electric energy harvester," *IEEE Transactions on Circuits and Systems I*, vol. 53, no. 2, pp. 288-295, Feb. 2006.
[45] E.O. Torres and G.A. Rincón-Mora, "Electrostatic energy harvester and Li-Ion charger for micro-scale applications," *Proc. IEEE Midwest Symposium on Circuits and Systems (MWSCAS)*, pp. 65-69, 2006.
[46] The MOSIS Service: AMI Semiconductor 1.50 Micron ABN Process [Online] Available: http://www.mosis.com/products/fab/vendors/amis/abn/.
[47] PowerStream [Online] Available: http://www.powerstream.com/thin-lithium-ion.htm.

Erick O. Torres (GS'05) was born and raised in San Juan, Puerto Rico. He received the B.S. degree from the University of Central Florida, Orlando, FL, and the M.S.E.E. degree from the Georgia Institute of Technology, Atlanta, GA, in 2003 and 2006, respectively, all in electrical engineering. Currently, he is working toward the Ph.D. degree in Electrical Engineering at the Georgia Institute of Technology in Atlanta, GA, where he is a research assistant at the Georgia Tech Analog, Power, & Energy IC Design Lab. He has been awarded several fellowships, including the Goizueta Foundation Fellowship, Georgia Tech President's Fellowship, and Texas Instrument's Analog Fellowship. Additionally, during a six-month co-op assignment in 2006, he worked as a circuit design engineer with Texas Instrument's Mixed-Signal Automotive group designing several analog circuit blocks for various integrated power control unit projects. His research interests include low-energy analog and power IC design for energy harvesters in micro-scale self-sustaining systems.

Gabriel A. Rincón-Mora (S'91-GS'92–M'97–SM'01) received his B.S., M.S., and Ph.D. in Electrical Engineering. He worked for Texas Instruments in 1994-2003, was appointed Adjunct Professor for Georgia Tech in 1999-2001, and became a full-time faculty member in 2001. His scholarly products include 5 books and 1 book chapter, 26 patents, over 100 scientific publications, and 26 commercial power management chip designs. He received the "National Hispanic in Technology Award" from the Society of Professional Hispanic Engineers, the "Charles E. Perry Visionary Award" from Florida International University, a "Commendation Certificate" from the Lieutenant Governor of California, an IEEE Service Award from IEEE CASS MWSCAS, and "Orgullo Hispano" and "Hispanic Heritage" awards from Robins Air Force Base. He was inducted into the "Council of Outstanding Young Engineering Alumni" by Georgia Tech and featured on the cover of Hispanic Business Magazine as one of "The 100 Most Influential Hispanics," La Fuente (Dallas publication), and three times on Nuevo Impacto (Atlanta magazine). He was a Florida Undergraduate Scholar and a Florida International University Faculty Scholar.

Dr. Rincón-Mora is (was/has been) an Associate Editor for IEEE's Transactions on Circuits and Systems II (TCAS II) since 2007; Circuit Design Vice Chair for IEEE's 2008 7th International Caribbean Conference on Devices, Circuits and Systems (ICCDCS); Chairman of Atlanta's joint IEEE Solid-State Circuits Society (SSCS) and Circuits and Systems Society (CASS) since 2005; member of IEEE's CASS Analog Signal Processing (ASP) Technical Committee since 2003; Steering Committee Member for IEEE's Midwest Symposium of Circuits and Systems (MWSCAS) since 2006; Technical Program Chair for IEEE's 2007 Joint MWSCAS-NEWCAS in Montreal; Technical Program Co-Chair for IEEE's 2006 MWSCAS in Puerto Rico; Vice Chairman of Atlanta's SSCS-CASS in 2004; and Selection Committee Review Panelist for the National Science Foundation (NSF) for 2003-2007. Dr. Rincón-Mora is a Senior Member of IEEE, a Life Member of the Society of Hispanic Professional Engineers (SHPE), and a Professional Member of IET. He is also a member of Eta Kappa Nu, Phi Kappa Phi, and a Life Member of Tau Beta Pi.